Theoretical Study of Hydroxylated and Dehydroxylated Surfaces of a Cristobalite Model of Silica

F. Vigné-Maeder* and P. Sautet

Institut de Recherches sur la Catalyse, CNRS, 2 av. Albert Einstein, 69626 Villeurbanne Cedex, France, and Ecole Normale Supérieure de Lyon, 46 allée d'Italie, 69361 Lyon Cedex 07, France

Received: December 6, 1996; In Final Form: May 14, 1997[⊗]

The (100) face of β-cristobalite covered by geminal hydroxyls has been taken as a model for the silica surface in order to describe the hydrogen bonding and the condensation of the surface hydroxyls of silica. Periodic Hartree−Fock calculations have been performed for slabs of five atomic layers. The optimized orientation of the hydroxyls corresponds indeed to hydrogen bonds at the surface. As a result, the surface atoms are slightly more negative and the hydroxyls have a specific orientation: one pointing outside the surface plane and the other one directed toward the bulk. The H-bond energy is evaluated to 25 kJ·mol^{-1}. The dehydration, leading to siloxane bridges, is endothermic by ≈200 kJ·mol^{-1}. It must be accompanied by a surface restructuring implicating more than only the first silicon and oxygen layers.

Introduction

In spite of numerous experimental studies of hydroxyl groups on the surface of silica, there are only limited theoretical descriptions of the surface structure, essentially in relation to adsorption properties. Interaction with small molecules, especially water, has been considered by using silanol, H_3SiOH, or orthosilisic acid, $Si(OH)_4$, as a model of isolated hydroxyl.[1,2] Larger surface models have been only taken into account in calculations using semiempirical potentials.[3,4] The purpose of the present paper is to provide a better insight into two aspects of the surface structure of silica: (1) the hydrogen bonding between surface hydroxyls and (2) the surface dehydroxylation leading to oxygen bridges. The calculations are performed at the Hartree−Fock level, for the model clusters (GAUSSIAN program) as well as for the infinite slabs or chains (CRYSTAL program). Correlation energies have been a posteriori estimated through a density functional approach.

A fully hydroxylated surface is obtained by treatment under vacuum at 120−150 °C, which removes physically adsorbed water. The surface density of OH groups is then nearly constant and does not depend in a significant way on the type of silica.[5] It amounts to about 5 ± 1 OH per nm^2. These surface OH groups are classified into several types. While the ^{29}Si-NMR technique[6−8] can measure the ratio of geminal hydroxyls (attached pairwise to the same silicon atom) to single ones, IR studies[9−11] permit one to distinguish hydrogen-bonded hydroxyls from isolated ones. Both techniques have been complemented by other methods, including chemical modifications[7,10] or adsorption properties analysis.[12,13] It has been found that on a fully hydroxylated silica surface nearly all the OH groups (80−90%) are hydrogen bonded[10,11] and 15−30% are of geminal type.[6−8]

Since bulk density and refractive index studies suggested[14] that the structure of amorphous silica is close to that of the β-cristobalite or similar crystalline phases, segments of hydroxylated surfaces have been modeled by (111) and (100) faces of β-cristobalite.[8] Not one of them gives a completely adequate description of the surface. The OH groups on (111) faces are of the single type, and the density is 4.55 OH per nm^2, which is close to experimental values. However, the distance between the OH groups is too large to allow hydrogen bonding, which is not consistent with the experimental results. On the (100) faces the hydroxyl groups can be hydrogen-bonded, but they are all of geminal type and the density is too large (7.9 OH per nm^2). In the present work we focused our study on the (100) faces, which can serve as a model for the hydroxyl groups that are both geminal and hydrogen bonded, keeping in mind that they cannot exclusively represent the whole surface of amorphous silica.

Dehydroxylation proceeds in different stages. Above 200 °C silanols Si−OH start to condense, forming siloxane bonds Si−O−Si and releasing water. The hydrogen-bonded hydroxyls are eliminated first. At 500 °C the density is 1−2 OH per nm^2 with virtually only isolated hydroxyls. The ratio of geminal and single OH groups does not vary significantly with temperature. At 500 °C they are both reduced by half. Above 900 °C hydroxylation implies stronger surface reconstruction, and rehydration becomes increasingly inefficient. After having modeled hydrogen-bonded hydroxyls, we attempted to estimate the energy cost of the siloxane bridge formation occurring in the first step of the dehydroxylation, through condensation of hydrogen-bounded hydroxyls. Several degrees of constraints due to the bulk rigidity have been introduced. We examined also the possible hydrogen bonding between the resulting vicinal hydroxyls.

Methods

The calculations of the infinite slabs were performed at the Hartree−Fock level with the pseudopotential version of the CRYSTAL 92 program developed in Turin.[15,16] The pseudopotentials of Durand and Barthelat (D−B)[17] were used with the following specific basis sets. Molecular adapted basis sets, the PS-31G basis set for silicon[18] and the larger PS-41G for oxygen,[19] were taken as a starting point. The external exponents of the sp shells were reoptimized to 0.210 and 0.236 for Si and O, respectively. Polarization functions play a minor role in fully ionic systems, but their importance becomes larger with increasing covalent character of the bonds.[20] Calculations performed on quartz showed that they were necessary to find the stabilization of the α-structure with respect to the β-one.[21] In this work polarization functions were added with exponents of 0.637 and 0.604 for silicon and oxygen, respectively. For

[⊗] Abstract published in *Advance ACS Abstracts,* September 15, 1997.

S1089-5647(96)04012-6 CCC: $14.00

hydrogen a 21G basis set has been used.[22] The HF energy has been corrected for correlation by integrating the HF charge density with the functional of Perdew (P86).[23] This procedure has been shown to be highly effective for covalent systems. For example, it decreased the error on the binding energy of α-quartz from 27% for the pure HF calculation to 4% with the correction.[24]

The calculations of the molecular clusters have been performed by using the GAUSSIAN 92 program that allows geometry optimization with analytical gradient of the energy. The same basis sets and pseudopotential for oxygen as those of the periodic calculations have been used. As the GAUSSIAN 92 program does not allow the use of negative n_{kl} exponent values, the Hay−Wadt pseudopotential[25] has been adopted for silicon. For comparison, calculations of the smallest clusters have been also done with CRYSTAL 92 and D−B pseudopotentials. The energies of $Si(OH)_4$, calculated with D−B or Hay−Wadt pseudopotentials differ by 0.02 au, and this difference is nearly independent of the geometry. Energy minimization leads to the same conformation, so that we considered that the result of the geometry optimization is not very sensitive to the choice of silicon pseudopotential.

Models

The structure of β-cristobalite has been calculated with the CRYSTAL program.[26] The experimental results, earlier analyzed in the $Fd\,\bar{3}m$ space group, have been interpreted as corresponding to the average structure of domains of lower symmetry.[26] Therefore, the optimization has been performed in the tetragonal space group $I\,\bar{4}2d$ with Si in 4(a) and O in 8(d) crystallographic positions. Values of the cell parameters $c = 7.27$ Å and $a = c/k\sqrt{2}$ with $k = 1.04$ have been found. The x parameter for the 8(d) positions is -0.0896. These results are in good agreement with the experimental values $c = 7.13$[28]−7.17 Å,[29] $k = 1$, and $x = -0.09$. In the calculated structure the elongation of the $Fd\,\bar{3}m$ unit cell along c, corresponding to k larger than 1 in the $I\,\bar{4}2d$ space group, results in almost regular tetrahedra of oxygens around each silicon atom (angles OSiO of 110.6° and 108.9° as compared to 112.8° and 107.8° in the experimental structure with $k = 1$). The calculated structure therefore appears to be an adequate description of the local atomic arrangement.

As is usually done, the notation for the crystallographic planes refers to the cubic $Fd\,\bar{3}m$ group. To study the properties of (100) faces of cristobalite, a slab of five atomic layers (O−Si−O−Si−O) was constructed parallel to the (001) crystallographic plane, in such a way that the external surfaces consist of oxygen atoms. Due to the elongation of the unit cell along c, the slabs parallel to the "equivalent" (100) and (010) planes would be slightly different, but not sufficiently so that they would exhibit other properties. They have not been considered here. The "free" valence of the surface oxygen atoms, resulting from the truncation of the crystal, was saturated with one hydrogen atom, which finally yields surfaces covered by geminal hydroxyls on each side of the slab. The five-layer slab appears as infinite chains simply placed side to side without covalent bonding between them, as is illustrated in Figure 1a. The links between these chains would be provided by lower layers. For the surface hydrogen-bond study, the positions of hydroxyl groups only were optimized: silicon atoms and internal oxygen atoms were fixed at their bulk optimized positions. For the dehydrated surface with oxygen bridges, this approximation is not valid since an extensive relaxation takes place. Various levels of constrained optimizations have been compared. Unless explicitly mentioned, upper and lower surfaces of the slab were considered equivalent and related by at least one symmetry operator.

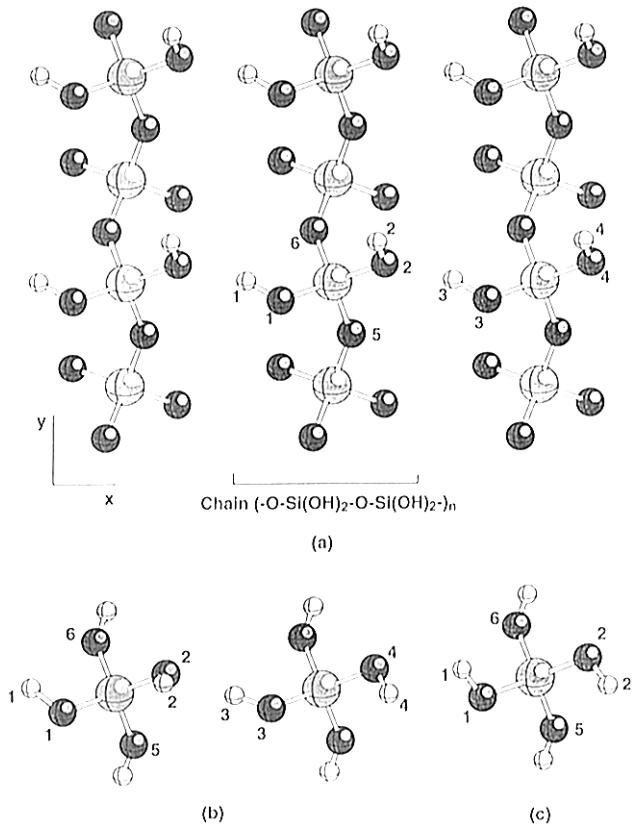

Figure 1. Different models represented in their optimal geometry: (a) a part of the fully hydroxylated slab (the hydrogen atoms at the bottom are not represented) with the chain $(-O-Si(OH)_2-O-Si(OH)_2-)_n$; (b) the $(Si(OH)_4)_2$ dimer; (c) The $Si(OH)_4$ cluster. Dark balls are oxygen, large grey balls silicon, and small white balls hydrogen atoms.

For comparison and discussion $(-O-Si(OH)_2-O-Si(OH)_2-)_n$ chains (Figure 1a) and $Si(OH)_4$ clusters (Figure 1c) are also considered, in which oxygen and silicon atoms have the same positions as in the slab. In the $Si(OH)_4$ cluster the hydrogen atoms that replace the silicon atoms of the bulk are fixed in the direction of those Si atoms and at the standard O−H distance of 0.955 Å.

Hydrogen Bonding

As emphasized in a recent review,[30] a hydrogen bond is not simple to define. It will be said here that hydrogen bond occurs between hydroxyl groups when they adopt a specific orientation with a binding energy larger than typical van der Waals interaction (>8 kJ/mol) and an H···OH distance smaller than the sum of the van de Waals radii (2.7 Å). The energy of each system is calculated as a function of the dihedral angles $\beta_n = H_nO_nSi\ z$ that govern the respective orientation of hydroxyl groups labeled in Figure 1. $\beta_n = 0°$ or 180° corresponds to hydroxyl groups perpendicular to the surface, toward the outside or the inside of the bulk, respectively. The angles are varied by steps of 40°, and the results are reported on contour diagrams. Geometry at the energy minima is then more precisely optimized (Table 1).

In the slab, hydroxyls are all of vicinal and geminal type at once, and, due to the chosen unit cell that contains two silicon atoms, they are not independent; for example, hydroxyls O_1H_1 and O_4H_4 are equivalent to O_3H_3 and O_2H_2, respectively (Figure 1a), so that the values of the dihedral angles β_2 and β_3 govern the orientation of all hydroxyls of the upper and lower surfaces. The main features of the energy contour map of Figure 2 are (a) the symmetry with respect to the diagonal due to the C_2 rotation axis passing through the silicon atoms and perpendicular

TABLE 1: Optimized Geometries of the Systems Considered in Figures 1 and 6[a]

	before optimization	monomer	chain	dimer	chain A	slab	chain B
β_n		71.5	77	(2) 12	(2,4) 2	(2,4) −50	(2) −54
				(3) 134	(1,3) 129	(1,3) 125	(3) 122
				(1) 103			(1) 100
				(4) 53			(4) 80
H_nO_nSi	118	118.6	117.7	(2) 118		(2,4) 117	
				(3) 119		(1,3) 122	
$O_nSi\ z$	55.33	56.2	56.3	(2) 54.0	(2,4) 53.5	(2,4) 54.5	(2) 53.9
				(3) 53.2	(1,3) 52.7	(1,3) 52.5	(3) 53.9
				(1) 57.4			(1) 57.1
				(4) 54.9			(4) 57.2
$O-H_n$	0.955			(2) 0.958			
				(3) 0.961			
$Si-O_n$	1.597			(2) 1.602			
				(3) 1.610			

[a] Lengths in Å, angles in deg. The values before optimization are those of the bulk of cristobalite. Atoms are indicated in parentheses (*n*) as in Figure 1. Some parameters have not been optimized when their variations yield very small changes in the dimer energy.

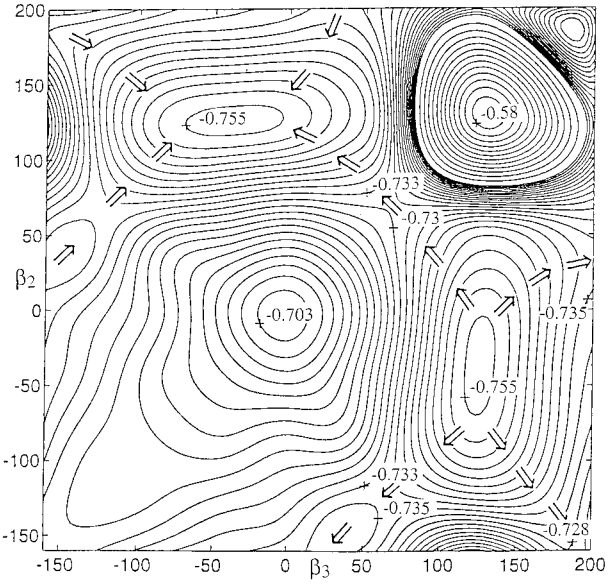

Figure 2. Energy map for the slab as function of the dihedral angles of the vicinal hydroxyls. The energy (au) is related to one pattern $-O-Si(OH)_2-O-Si(OH^*)_2-$ where the hydroxyl groups $(OH)_2$ and $(OH^*)_2$ are located on the upper and lower surface, respectively, and are equivalent by symmetry. The energy is shifted by 104 au, and the contours are separated by 0.0025 au. All four possible paths for the exchange H_3-H_2 in the hydrogen bond are represented.

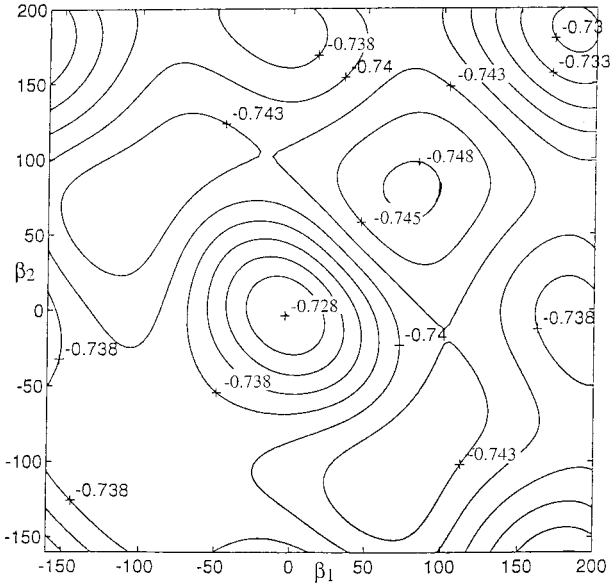

Figure 3. Energy map for the chain $(-O-Si(OH)_2-O-Si(OH^*)_2-)_n$ as a function of the hydroxyl dihedral angles. As in the Figure 2, energy is shifted by 104 au, and contours are separated by 0.0025 au.

to the surface, (b) a very large energy maximum for $\beta_2 = \beta_3 = 130°$, (c) a lower maximum for $\beta_2 = \beta_3 = 0°$, and (d) two energy minima for different values of these angles, $\beta_2 = -40°$ and $\beta_3 = 130°$ (as shown in Figure 1a) or vice versa. Are these extrema related to interactions between geminal hydroxyls (like O_1H_1 and O_2H_2 in Figure 1a) or to interactions between vicinal hydroxyls (like O_2H_2 and O_3H_3)? This is easily elucidated for the maxima since they can be related to simple steric hindrance between the hydrogen atoms of geminal hydroxyls for $\beta_2 = \beta_3 = 0°$ (distance $H_1-H_2 = 2.4$ Å) and between the hydrogen atoms of vicinal hydroxyls for $\beta_2 = \beta_3 = 130°$ (distance $H_2-H_3 = 0.8$ Å). For the minima, there is evidence of an interaction of hydrogen-bonding type between vicinal hydroxyls since one hydroxyl, O_3H_3 for $\beta_3 = 130°$, points toward the oxygen atom of its vicinal hydroxyl, O_2, at a distance of 1.73 Å, which is lower than the sum of the van der Waals radii, 2.7 Å. This optimal orientation is more rigid for the hydrogen atom H_3 involved in the hydrogen bond since an energy of 3 kJ·mol^{-1} per bond yields fluctuations of ±30° for β_2 and only ±10° for β_3. Consequently going from one minimum to the other by exchange of H_3 and H_2 in the hydrogen bond is difficult; a rather large energy barrier of 33 kJ·mol^{-1} needs to be overcome for whatever path of minimal energy is indicated on Figure 2. In the following the hydroxyls O_2H_2 and O_3H_3 in the structure of Figure 1a will be described as free and bound hydroxyls, respectively.

To confirm these observations, a model without vicinal interactions, i.e. a single chain, has been considered. The energy contour map (Figure 3) looks very different from the previous one. It is smoother, the very high extremum at $\beta_2 = \beta_3 = 130°$ is removed, and a maximum at $\beta_2 = \beta_3 = 180°$ appears, similar to the $\beta_2 = \beta_3 = 0°$ situation. The dissymmetric minima have disappeared and are replaced by a single minimum for $\beta_2 = \beta_3 = 77°$, where a transition state was found between hydrogen-bonded minima in the case of the complete slab. This confirms that the large maximum on Figure 2 is due to steric interaction between vicinal groups, while interchain hydrogen bonding controls the preferred orientation of the surface hydroxyls. An optimal geometry close to that of the single chain is also obtained for the $Si(OH)_4$ cluster (Table 1), but it differs from the fully optimized geometry where $Si(OH)_4$ adopts the S_4 symmetry with the dihedral angle of all hydroxyls equal to 32°[31] or 37°;[32] this is because the lower hydroxyls in the cluster are imposed to have the same orientation as the corresponding O−Si of the bulk (dihedral angles of 78.47°). It can be verified that geminal hydroxyls are not linked by hydrogen bonding: the

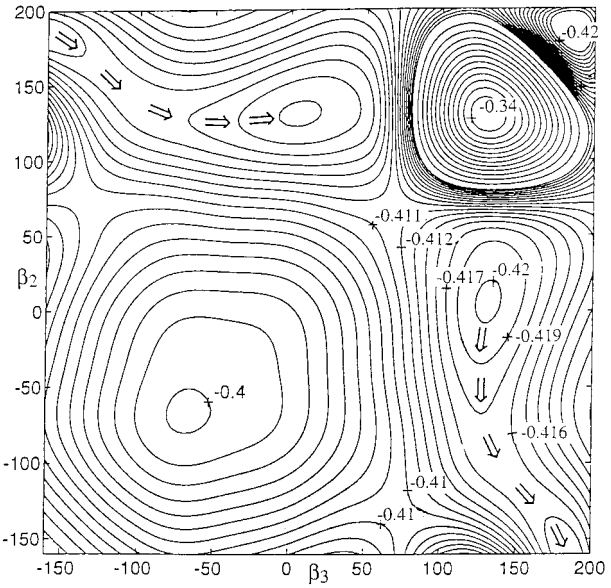

Figure 4. Energy map for the dimer $(OH)_3Si-OH\cdots OH-Si(OH)_3$ as a function of the dihedral angles of the vicinal hydroxyls. The hydrogens at the bottom are kept in the position modeling the bulk of silica, and each external hydroxyl has the best orientation with respect to its geminal hydroxyl. Energy is relative to one H-bond so that it is shifted by 138 au, and the contours are separated by 0.00125 au. Arrows represent the path of minimal energy for the substitution of H_3 by H_2 in the hydrogen bond.

$H_1\cdots O_2$ and $H_2\cdots O_1$ distances are large (3.03 Å), and the rotation of one of the hydroxyls around the Si-O bond, the other one keeping the $\beta = 77°$ orientation, only shows a barrier of 7 kJ·mol^{-1}. Therefore, intrachain interactions of hydroxyls are not very important.

Thus it is the interaction between two adjacent chains that is at the origin of the orientation of the surface hydroxyls of the slab. Is this orientation only given by a local interaction between two hydroxyls, or is it also influenced by the infinite character of the system? The first possibility can be examined with the model composed of two $Si(OH)_4$ at the same distance as in the bulk (Figure 1b). Identical results concerning the orientation have been obtained with the larger model composed of two $(OH)_3Si-O-Si(OH)_3$ for which the inner atoms are frozen as in the slab. In Figure 4 the energy contour map corresponding to the variation of the dihedral angles of the vicinal hydroxyls is reported. In comparison with Figure 2 the strong repulsion between the geminal hydroxyls ($\beta_2 = \beta_3 = 0°$) has disappeared because in that case the external hydroxyls O_1H_1 and O_4H_4 are independently optimized and are not forced to follow the rotation of O_3H_3 and O_2H_2 groups, respectively (they are roughly parallel to the modeled surface). As in case of the slab, we find the two minima interpreted as hydrogen bonding ($\beta_2 = 12°$, $\beta_3 = 134°$, and vice versa), but the energy barrier for the H_2-H_3 exchange in the hydrogen bond is lower. It amounts only to 13 kJ·mol^{-1} for the minimal energy path indicated with the arrows in Figure 4, and the geometry of the transition state corresponds to both hydroxyls directed toward the bulk, e.g. at $\beta_2 = 180°$ and $\beta_3 = -180°$, or equivalently $\beta_2 = \beta_3 = 180°$. Another difference is the orientation of the "free hydroxyls", which is here nearly perpendicular to the surface ($\beta_2 = 12°$ instead of $-50°$). This cannot be attributed to the interaction between geminal hydroxyls since the external hydroxyls are free to rotate.

Therefore the dimer model gives a correct qualitative picture of the hydrogen bond, but it fails to accurately reproduce both the strength and geometry of that interaction. More extended models are then required. In order to understand the origin of the geometry difference between the slab and the dimer, two infinite periodic chains have been considered (Figure 5), directed along *x* and *y*. Chain A, along *x*, is built with monomers $HO-Si(OH)_2-O-Si(OH)_2OH$ linked together by hydrogen bonds. Chain B, along *y*, consists of two simple chains linked by hydrogen bonds. The orientation of the free hydroxyl strongly depends on the chosen model, chain A giving a result close to that of the isolated dimer, while chain B yields an orientation similar to that of the full slab. Then, the hydrogen bonding mainly comes from local interactions, but long range interactions from infinite models influence the precise geometry.

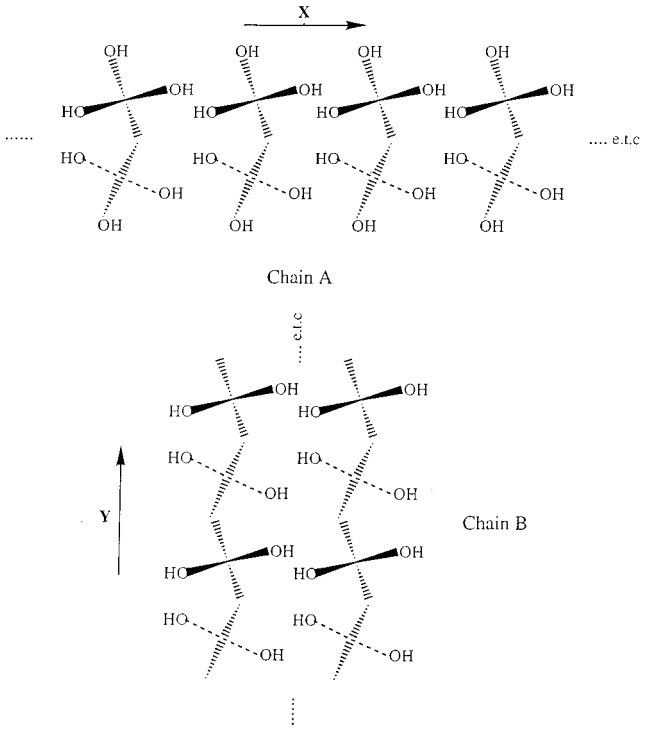

Figure 5. Two chains with hydrogen bonds in single file (A) or located side to side (B).

TABLE 2: Hydrogen Bond Energy in the Different Models of Silica Surface, in kJ·mol^{-1} [a]

	H−F level	with correlation
(1) $(H_2O)_2$	−21.2[b]	−27[b]
	−21.3[c]	−25.3[c]
(2) $(Si(OH)_4)_2$	−3.4	−14
(3) $(Si(OH)_4)_n$	−8.6	−21
(4) $((OH)_3Si-O-Si(OH)_3)_2$	−9.5	−20
(5) chain A	−13.9	−26
(6) chain B	+3.8	−9
(7) slab	−13.9	−25

[a] Values for the water dimer are indicated for comparison. Correlation corrections are estimated through the density functional procedure of Perdew.[23] [b] Calculated with the same basis sets and pseudopotential as for the models of silica. [c] Reference 35. These calculations use a 6−31+G(d,p) basis and the fourth-order Moller−Plesset perturbation theory for the correlation energy.

The strength of the hydrogen bonding is generally discussed in relation to the binding energy of the molecular association, defined as the energy difference between dimer and monomers, in their optimized geometry. This is generally not well appropriate to the hydrogen bond formation on a surface because separated systems are not clearly defined. However, for our model surface, the covalent bonds leading to the bulk formation are not included and subunits exclusively linked by hydrogen bonding appear in a natural way. Therefore the binding energies, collected in Table 2, correspond to the usual definition. The correlation energy, estimated through a density functional, is nearly identical for all systems. It amounts to about −12 kJ·mol^{-1}, which can represent more than 50% of the total

TABLE 3: Mülliken Atomic Charge Distributions in the Different Models of Figures 1 and 6[a]

	systems with H-bonding				systems without H-bonding	
atom	slab	chain A	chain B	dimer	chain	$Si(OH)_4$
O_3	−1.06	−1.07	−1.06	−1.07	−1.02	−1.01
H_3	0.47	0.47	0.46	0.47	0.45	0.44
O_2	−1.03	−1.03	−1.01	−1.03	−1.02	−1.01
H_2	0.46	0.46	0.46	0.46	0.45	0.44
Si	2.32	2.34	2.31	2.34	2.31	2.33
O_5	−1.17	−1.16	−1.17	−1.04	−1.17	−1.04

[a] The hydrogen bonding is $O_2\cdots H_3-O_3$.

energy. Compared to the case of the water dimer, the hydrogen bond between surface hydroxyls is always weaker, because the surface introduces a constraint that prevents hydroxyls from adopting an optimal position. From the various models given in Table 2, it can be seen that the description of the surface inner layers, by simple H endings (lines 2 and 3 in Table 2) or with another $Si(OH)_2$ layer (lines 4 and 5 corresponding to 2 and 3, respectively), influences the strength of the hydrogen bonding. A better description of the inner layers increases the binding energy by about 50%. The bond energy also depends on the long range interactions from periodic repetition of hydrogen bonds. When the system is periodic in the direction perpendicular to the H-bond (chain B) the energy is markedly small, even positive at the Hartree−Fock level. However the energy is the same as in the slab case if the repetition is in the perpendicular direction (chain A). Therefore hydrogen bonding can be very sensitive to the surrounding, and in particular, bonds aligned in single file are energetically favored with respect to bonds located side by side. This can be interpreted by a very crude electrostatic model in which dipoles are preferentially aligned rather than side by side. Compared to the slab, agreement in the H-bond energy or geometry is obtained with a different chain model.

A first insight in the charge distribution on the surface is given by the Mülliken electronic population analysis. Total charges are reported in Table 3 for the different models. In all the cases the hydrogen bond formation results in larger charges on the surface hydrogen and oxygen atoms, especially on the oxygen atom O_3 of the hydrogen bond, with a negative charge increased in absolute value by 0.05 with respect to that of $Si(OH)_4$. As expected, the oxygen atoms of the bulk are not well described in the dimer and $Si(OH)_4$ because they are linked to hydrogen instead of silicon. Their charges are about −1.04 to be compared with −1.17 in the slab and −1.16 in the crystal. Despite the crudeness of the Mülliken description, it can be qualitatively concluded that hydrogen bonding increases the polarization of the surface hydroxyls.

Dehydroxylation

Reversible dehydroxylation of silica occurs by heating between 200 and 900 °C. This variation of temperature indicates that the reaction becomes more and more difficult during the dehydration, due to the modification of the surface. Assuming an outgassing pressure of 10^{-3} Pa and taking into account the entropy of water, simple thermodynamics calculations give an enthalpy of reaction increasing roughly from 150 to 300 kJ per mol of water during the dehydration. In a molecular approach the reaction can be modeled by the condensation of two orthosilicic acid molecules

$$2Si(OH)_4 \rightarrow (HO)_3Si-O-Si(OH)_3 + H_2O$$

The energy of the molecules participating in the reaction have been recently obtained through full electron calculations with the 6-31G* and the large MC6-311G** basis sets, at the Hartree−Fock or second-order perturbation (MP2) level.[31−34] With both basis sets the energy differences yield negative bridge formation energies, −20 and −30 kJ·mol^{-1} without and with correlation, respectively (i.e. exothermic reactions, Table 4). These results correspond to fully optimized free molecules allowing intramolecular hydrogen bonding in the dimer. They cannot be related to the oxygen bridge formation on real surfaces because they do not take into account the constraints that would be exerted by the solid on the geometry of the model molecules. The interest of the periodic systems used in this work would be to introduce this constraints in a natural way and for different degrees of dehydration. In actual fact, owing to the unit cell size limitation, only one possible half-dehydrated silica surface has been considered. Half of the hydrogen bonds were replaced by oxygen bridges, so that each surface silicon atom was bonded to one hydroxyl and to the oxygen of a bridge (instead of two hydroxyls), leading to an hydroxyl coverage of 4 OH/nm^2 (Figure 6a). In the five atomic layer slab considered above for the calculations, this results in quasi-independent double chains. Two symmetrical bridges, one on each surface of the slab, can be considered in the unit cell (Figure 6b), or at the expense of a less symmetrical calculation, a single O bridge on the upper surface can be modeled (Figure 6c).

Such a formation of a Si−O−Si bridge on the surface requires an important surface relaxation that needs to be included in the calculation in order to obtain realistic reaction enthalpy. The constraints imposed by the bulk inner layers, not included in the slab models, must also be taken into account. Two levels of relaxation have been considered, and the results are summarized in Table 4 for the energy of formation of the siloxane bridge and in Table 5 for the geometry and the atomic charges. In a first step (model I), bridge oxygen atom, neighbor silicon

TABLE 4: Energies of the Systems Involved in the Reaction of Formation of the Siloxane Bridge 2RSi−OH → RSi−O−SiR + H_2O[a]

	RSi−OH	RSi−O−SiR	H_2O	$\Delta_r E$
molecular models: R = $(OH)_3$				
6-31G* (H−F)	−590.825 56[b]	−1105.674 75[b]	−75.983 92[b]	−0.007 55 (−20)
MC6-311G* (H−F)	−591.024 3[c]	−1106.010 62[c]	−76.046 31[d]	−0.008 31 (−22)
MC6-311G* (MP2)	−592.117 2[c]	−1107.962 85[c]	−76.282 87[d]	−0.011 27 (−30)
slab model (I)	−52.379 54	−87.710 47	−16.880 08	0.169 (442)
	[−53.347 22]	[−89.315 75]	[−17.184 95]	[0.194 (508)]
cluster model I	−69.231 17	−121.426 14	−16.880 08	0.156 1 (410)
R = $(OH)_3$	[−70.501 01]	[−123.637 94]	[−17.184 95]	[0.179 1 (470)]
slab model II	−104.759 08	−192.562 25	−16.880 08	0.075 84 (199)
	[−106.694 44]	[−196.111 78]	[−17.184 95]	[0.092 15 (242)]
cluster model II	−77.788 01	−138.655 60	−16.880 08	0.040 35 (106)
R = $(OH)(OSiH_3)_2$	[−79.438 90]	[−141.640 68]	[−17.184 95]	[0.052 17 (137)]

[a] The constraints imposed to the slab model are in a decreasing order from A to D. Energies in hartrees excepted for the value of $\Delta_r E$ in parentheses, in kJ·mol^{-1}. The values in brackets include the correlation correction. [b] Reference 34. [c] Reference 32. [d] Present work.

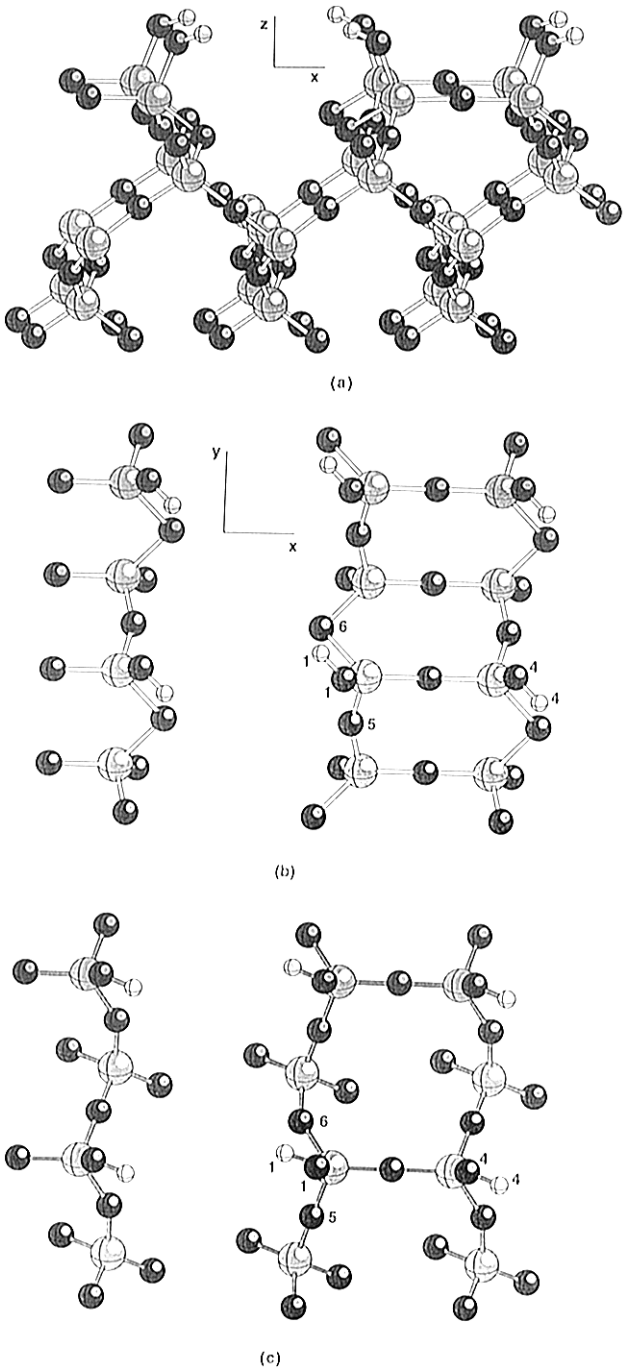

Figure 6. Views of he half-dehydroxylated silica surface: (a) with the bulk cut after the eighth atomic layer; (b) model slab of five atomic layers with symmetric dehydroxylation; the internal oxygen atoms 5, 6 are fixed at the same position as in the bulk (model I); (c) five atomic layer slab with dehydroxylation on the upper surface only (model II). The hydrogen atoms at the bottom are not represented.

and hydroxyl groups positions were optimized on the model of the symmetrical slab (Figure 6b). Positions of the third layer O_5 and O_6 atoms (as labeled in Figure 1a) were fixed to that of the bulk, and the cell parameters were not modified. With the CRYSTAL code, such geometry optimizations have to be performed manually. The formation energy for the siloxane bridge was calculated from the slab results and also from a related cluster model $(HO)_3Si-O-Si(OH)_3$ with identical atomic positions (see Table 4).

Average values of bond lengths and angles have been determined from different structures of silica. They are 1.63 Å for Si−O, 144° for Si−O−Si, and 109.5° for O−Si−O.[36] The energy costs associated to deviations from these values have been estimated through molecular calculations:[37] the Si−O−Si angle can take values between 130° and 180° with an energy variation less than 20 kJ·mol^{-1}, but changing the Si−O bond length or the O−Si−O angle requires on the order of 130 kJ·mol^{-1} per 0.1 Å or 100 kJ·mol^{-1} per 10°. In model I the high formation energy can be attributed to the long Si−O bond in the bridge and to the distortion of the oxygen tetrahedra around the silicon atoms (Table 5). Moreover the internal Si−O−Si angles have unrealistic values (79° and 104° for O_6 and O_5, respectively (Figure 6b)), which results from the position of the internal oxygens as a link between both surfaces of the slab. Therefore it is necessary to extend the relaxation and optimize the position of third layer O_5 and O_6 atoms. This was done in model II and requires the use of the nonsymmetrical model of Figure 6c with only one dehydrated surface. In order to introduce the constraints from the bulk, fourth layer Si atoms have been kept fixed, and hence the 2D lattice parameters were not modified. From the low symmetry, the disk space for two electron integrals is in that case large (4.5 GB), which makes it difficult to extend the model further and also to perform a manual geometry optimization, taking into account the important number of degrees of freedom. As far as geometry is concerned, cluster models are known to give very reliable results. Therefore, the cluster model of Figure 7 was considered and optimized with the constraint of keeping the SiH_3 termination groups fixed at positions and orientations relative to the bulk structure. The optimal geometry was then transferred into the slab structure, and a single-point energy was calculated. As before, the siloxane bridge formation enthalpy was calculated from both the cluster and slab energies.

TABLE 5: Geometry of the Bridge and Mülliken Atomic Charge Distribution in the Different Models of Dehydroxylated Surface (Lengths in Å, Angles in deg)[a]

	mean[b]	model I	model II
$Si-O_b$	1.63	1.71	1.62
$Si-O_b-Si$	144[c]	178	172
$OH-Si-O_b$	109	109	108
O_6-Si-O_b	109	129	119
O_5-Si-O_b	109	102	105
O_5-Si-O_6	109	96	104
bridge q_O		−1.22	−1.18
hydroxyl q_O		−1.00	−0.99
hydroxyl q_H		0.46	0.44
q_{Si}		2.24	2.33
mean (q_{O_5},q_{O_6})		−1.10	−1.18

[a] O_b is the bridge oxygen atom and labels refer to Figure 6b,c. [b] Reference 36. [c] Si−O−Si in the bulk.

The strain in Si−O−Si is much better released from the relaxation of model II compared to model I (see Table 5). The Si−O bond distance is close to the mean value, and the environment of the Si atom is much more tetrahedron-like. The larger angular displacement is for O_6-Si-O_{bridge}, and it is clear from Figure 7b that O_6 has the larger lateral displacement in the optimization. The Si−O−Si angle at the bridge remains larger than the bulk mean value, and the oxygen surprisingly moves slightly inward compared to the Si−Si direction. The reaction enthalpies of course decreased compared to model I, and the calculated endothermicity (200 kJ·mol^{-1}) compares well with the thermodynamics estimate. The inclusion of correlation corrections increases the endothermicity by 30−60 kJ·mol^{-1}. Compared to the related cluster models, the slab models always yield a more positive formation energy. It is clear that the values from model II still represent an upper bound for this reaction enthalpy, not taking into account the error from the quantum chemical approximation. It would be reduced by an optimization of the fourth layer Si atoms. However, these Si atoms are bonded to three inner oxygen atoms, and displacement are hence difficult at these centers. This is why additional relaxation

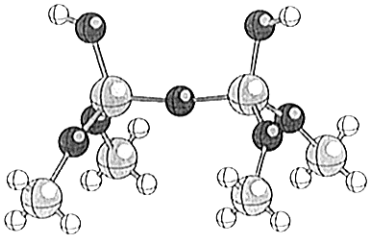

(a)

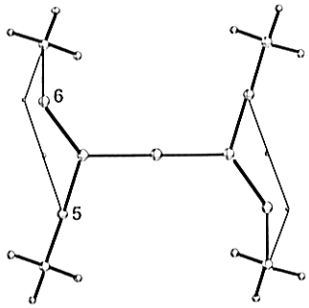

(b)

Figure 7. Cluster selected for the geometry optimization of slab model II of the dehydroxylated surface. SiH_3 groups are kept fixed: (a) side view, (b) simplified top view showing the extent of the relaxation (thick lines) compared to the fully hydroxylated surface (thin lines).

should be small and the enthalpy values from model II can be considered as realistic estimates. Mülliken atomic charges are reported in Table 5. The bridge formation yields surface oxygens that are markedly more negative (about −1.2, similar to that of bulk oxygens) and hydroxyls that have lost the polarization due to hydrogen bonding.

Conclusion

The distance between two pairs of geminal hydroxyls on the (100) face of β-cristobalite is small enough to readily allow hydrogen bonding between two vicinal hydroxyls. The angle (O···H−O) = 160°, the distance O···H = 1.70 Å, and the formation energy of 25 kJ·mol^{-1} are in agreement with such interactions. Hydrogen bonding formation results in a surface exposing hydrogen atoms belonging to hydroxyls nearly free to rotate from the position perpendicular to a position parallel to the surface, and oxygen atoms belonging to bound hydroxyls directed toward vicinal surface oxygen atoms. Mülliken atomic net charges are 0.47 and −1.06 e, respectively. The geometric conformation arising from surface hydrogen bonding would make easier an electrophilic attack on these oxygen atoms that point a lone pair out of the surface. All the models used for this theoretical approach and which include vicinal hydroxyls present a similar hydrogen bond, but an appropriate description of the inner surface layers and the long range interactions from periodic repetition along one or two directions modify in some extend the geometry or the energy of the bond. This shows that an accurate description of the surface hydrogen bond cannot be obtained from calculations on small clusters.

In contrast with free molecular models that result in an exothermic reaction, the siloxane bridge formation energy has been found positive for all slab models. The strains in the siloxane bridge impose a significant restructuring of the surface. An atomic optimization up to the second neighbor atom of the oxygen bridge needs to be considered in order to obtain reasonable formation energies. Fully optimized small clusters are not able to reproduce the geometric constraints imposed by the surface inner layers on the displacement of surface atoms and are not appropriate for a description of the surface reaction.

References and Notes

(1) Pelmenschikov, A. G.; Morosi, G.; Gamba, A. *J. Phys. Chem.* **1992**, *96*, 7424.
(2) Garrone, E.; Ugliengo, P. *Langmuir* **1991**, *7*, 1409.
(3) Valencia, E. *J. Chem. Soc., Faraday Trans.* **1994**, *90*, 2555.
(4) Shay, T. B.; Hsu, L.-Y.; Basset, J.-M.; Shore, S. G. *J. Mol. Catal.* **1994**, *86*, 479.
(5) Zhuravlev, L. T. *Langmuir* **1987**, *3*, 316.
(6) Léonardelli, S.; Facchini, L.; Fretigny, C.; Tougne, P.; Legrand, A. P. *J. Am. Chem. Soc.* **1992**, *114*, 6412.
(7) Tuel, A.; Hommel, H.; Legrand, A. P. *Langmuir* **1990**, *6*, 770.
(8) Sindorf, D. W.; Maciel, G. E. *J. Am. Chem. Soc.* **1983**, *105*, 1487.
(9) Marrow, B. A.; McFarlan, A. J. *J. Phys. Chem.* **1992**, *96*, 1395.
(10) Van Der Voort, P.; Gillis-D'Hamers, I.; Vansant, E. F. *J. Chem. Soc., Faraday Trans.* **1990**, *86*, 3751.
(11) Van Der Voort, P.; Gillis-D'Hamers, I.; Vrancken, K. C.; Vansant, E. F. *J. Chem. Soc., Faraday Trans.* **1991**, *87*, 3899.
(12) Gillis-D'Hamers, I.; Cornelissens, I.; Vrancken, K. C.; Van Der Voort, P.; Vansant, E. F. *J. Chem. Soc., Faraday Trans.* **1992**, *88*, 723.
(13) Bolis, V.; Fubini, B.; Marchese, L.; Martra, G.; Costa, D. *J. Chem. Soc., Faraday Trans.* **1991**, *87*, 497.
(14) Iler, R. K. *The Colloid Chemistry of Silica and Silicates*; Cornell University Press: Ithaca, NY, 1955; pp 242−247.
(15) Pisani, C.; Dovesi, R.; Roetti, C. *Lecture notes in chemistry*; Springer Verlag: Heidelberg, 1988, Vol. 48.
(16) Dovesi, R.; Saunders, V. R.; Roetti, C. *CRYSTAL 92. User documentation*; University of Torino: Torino, and SERC Daresbury Laboratory: Daresbury.
(17) Durand, P.; Barthelat, J. C. *Theor. Chim. Acta* **1975**, *38*, 283.
(18) Bouteiller, Y.; Mijoule, C.; Nizam, M.; Barthelat, J. C.; Daudey, J. P.; Pelissier, M.; Silvi, B. *Mol. Phys.* **1988**, *65*, 295.
(19) Bouteiller, Y. Private communication. Exponents of the four contracted Gaussian functions: 23.711 274, 6.226 854, 2.108 452, 0.706 472. Coefficients for the S basis: 0.016 944, −0.161 506, 0.112 376, 0.669 954. Coefficients for the P basis: 0.026 384, 0.115 073, 0.298 993, 0.470 880.
(20) Salasco, L.; Dovesi, R.; Orlando, R.; Causà, M. *Mol. Phys.* **1991**, *72*, 267.
(21) Silvi, B.; d'Arco, P.; Causà, M. *J. Chem. Phys.* **1990**, *93*, 7225.
(22) Binkley, J. S.; Pople, J. A.; Hehre, W. J. *J. Am. Chem. Soc.* **1980**, *102*, 939.
(23) Perdew, J. P. *Phys. Rev. B* **1986**, *33*, 8822.
(24) Dovesi, R.; Roetti, C.; Freyria-Fava, C.; Aprà, E.; Saunders, V. R.; Harrison, N. M. *Philos. Trans. R. Soc. London A* **1992**, *341*, 203.
(25) Hay, P. J.; Wadt, W. R. *J. Chem. Phys.* **1985**, *82*, 270; 284; 299.
(26) Vigné-Maeder, F.; Sautet, Ph. Unpublished results.
(27) O'Keefe, M.; Hyde, B. G. *Acta Crystallogr.* **1976**, *B32*, 2923.
(28) Wright, A. F.; Leadbetter, A. J. *Philos. Mag.* **1975**, *31*, 1391.
(29) Peacor, D. R. *Z. Kristallogr.* **1973**, *138*, 274.
(30) Aakeröy, C. B.: Seddon, K. R. *Chem. Soc. Rev.* **1994**, *22*, 397.
(31) Sauer, J. *J. Phys. Chem.* **1987**, *91*, 2315; *Chem. Rev.* **1989**, *89*, 199.
(32) Teppen, B. J.; Miller, D. M.; Newton, S. Q.; Schäfer, L. *J. Phys. Chem.* **1994**, *98*, 12545.
(33) Hess, A. C.; McMillan, P. F.; O'Keefe, M. *J. Phys. Chem.* **1987**, *91*, 1395.
(34) O'Keeffe, M.; Domengès, B.; Gibbs, G. V. *J. Phys. Chem.* **1985**, *89*, 2304.
(35) Frisch, M. J.; Pople, J. A.; Del Bene, J. E. *J. Phys. Chem.* **1985**, *89*, 3664.
(36) Gibbs, G. V. *Am. Mineral.* **1982**, *67*, 421.
(37) Michalske, T. A.; Bunker, B. C. *J. Appl. Phys.* **1984**, *56*, 2686.